Remediation of Contagious Metals from Mine-used Water using *Carica Papaya* Trunk Enhanced Charcoal produced with HCl acid

A. E. Adetoro[1,2*], S. O. Ojoawo[3]

[1]Department of Civil Engineering, The Federal Polytechnic, Ado-Ekiti, Nigeria.
[2]Department of Civil Engineering, Olabisi Onabanjo University, Ago-Iwoye, Nigeria.
[3]Department of Civil Engineering, Ladoke Akintola University of Technology, Ogbomoso, Nigeria.

ABSTRACT: Consumptions of contagious metals particularly from mine used water usually result in grievous health diseases and loss of aquatic lives. This research concentrated on elimination of specific contagious metals (Co^{3+}, Fe^{2+}, and Pb^{2+}) from mine used water using Carica Papaya Trunk Enhanced Charcoal produced with HCl (CPTEC – HCl). The contagious metals' concentrations of the mine used water, predominant functional classes and surface structure of the produced CPTEC-HCl were ascertained utilising some analytical techniques. The adsorption (batches) and desorption experiments applying six parameters were carried out. The suitability of the adsorption facts generated was conducted using adsorption isotherms, kinetics, and thermodynamics through linear and non-linear regressions with two error functions. The contagious metals' original values were higher than the acceptable requirements. After treatment, CPTEC-HCl eliminated the contagious metals completely (100%) using 0.516 g of the adsorbent with 0.028 mm granule-size at 146.576 rpm, 51.718 minutes, pH of 6.969 at 30 °C. The processes were majorly chemisorptions, largely followed Freundlich, Dubinin-Radushkevich isotherms, Pseudo-second-order kinetic models and highly influenced by the adsorption parameters. The adsorption processes were favourable, feasible, and natural. CPTEC-HCl is an excellent alternative adsorbent for commercial enhanced charcoal in contagious metals' elimination from real-world effluent especially mined used water.

KEYWORDS: Adsorption, Chemisorption, Desorption, Error functions, Linear and non-linear regression.

[Received: Dec. 20, 2023; Revised Aug 27, 2024; Accepted Sep 2, 2024] Print ISSN: 0189-9546 | Online ISSN: 2437-2110

I. INTRODUCTION

In mining industries, contagious metals are being released in higher proportion into the environment and water bodies, which results in the industries producing contagious metals for example cadmium, chromium, cobalt, copper, iron, lead, zinc, etc; some of the most dangerous amid the chemical-concentrated ones. Contagious metals could be absorbed by living creatures due to their high solubility in the water habitat. Consequently, substantial concentrations of contagious metals may accumulate in the human anatomy after they enter the food chain. Absorption of the metals above the permitted concentration can cause grievous health diseases. Therefore, it is of utmost importance to look for means of reducing or removing the contagious metals' concentration in the industrial effluents due to their high poisonous nature (Badamasi et al., 2021; Hadzi, 2022; Wiafe et. al., 2022; Minga et al., 2023).

Adsorption using Bioremediation (i.e. Biosorption) is at the forefront of the most recent methods sought after in remediating contagious metals from wastewater. The functional groups display on the contagious metal ions' outer surfaces compounded them through the substances' activity. It is an efficient and inexpensive method compared to the other wastewater treatment methods. Consequently, the most suitable method of treating large quantity and low concentration complex wastewaters (Kumaraiah et al., 2021; Samrot et al., 2021; Natani et al., 2022).

The efficiencies of low-priced adsorbents in contagious metals' elimination from industrial sewage are being broadly investigated to get affordable natural adsorbents that are simply obtainable and efficacious in poisonous metals' elimination from the wastewaters especially mining one. Generally, they have good adsorption capacity. These unorthodox natural adsorbents have other merits than being largely available in nature. Nearly all of them require little preliminary processing and are waste by-products from the other industry. Hence, they are replacements for more expensive adsorbents e.g. enhanced charcoal, synthetic polymers etc (Samrot et al., 2021; Idibie et al., 2021; Karn et al., 2021).

Enhanced Charcoals produced from agricultural bio-materials have been used recently to eliminate contagious metals from wastewater by many researchers as shown in Table 1 - this is a result of its affordability, accessibility, and efficacy (Kumaraiah et al., 2021). These include neem (Hatiya et al., 2022; Adetoro and Ojoawo, 2023), coconut (Umerah et

*Corresponding author: yemmieadyt@yahoo.com *doi:* http://dx.doi.org/10.4314/njtd.v21i4.2233

al., 2020; Packialakshmi et al., 2023), tea (Claude et al., 2022), Orange (Kumaraiah et al., 2021), Mango (ElNasri et al., 2022; Wang et al., 2022), Melon (Ahmadi et al., 2023), and Rice husk (Naik et al., 2023) among others.

Nonetheless, unlike the above previous works reviewed, there has not been a study done on the use of *Carica Papaya* Trunk Enhanced Charcoal (CPTEC) improved with HCl in contagious metals' remediation from mine used water. An extensive study on adsorption of three selected contagious metal ions (i.e. Co^{3+}, Fe^{2+}, and Pb^{2+}) from Igbeti marble Mine Used Water – MUW (i.e. real-life wastewater) using CPTEC produced with HCl enhancing agent was carried out. The selection of the three contagious metals is based on the previous works of Adetoro and Ojoawo (2023) among others, which shows possibilities of removing them without having effects on other contagious metals.

As can be seen in Table 1, *Carica Papaya* Trunk (CPT) is a better adsorbent than other agricultural biomaterials due to its high fixed charcoal and low moisture contents. According to Natania et al. (2022), it also has some secondary metabolites, demonstrating its ability to bind and adsorb metals. There were possibilities of using various adsorbents, but not CPTEC – HCl (An adsorbent / charcoal produced from *Carica Papaya* Trunk and then enhanced with HCl). Most of the adsorbents in the literature were produced from other agricultural bio-materials (Table 1), but not enhanced using HCl. Also, the ones produced using *Carica Papaya* were enhanced with other acids (e.g. H3PO4) and bases (e.g. NaOH, $ZnCl_2$), but not HCl acid.

This study aims at determining the quantities of specific contagious metals in the mine used water; determining the efficiency and suitability of CPTEC - HCl in eliminating the selected contagious metals from the mine used water. Batch adsorption experiments and some adsorption process models were used to attain these goals.

Table 1: Some adsorbents and their properties

Precursor material	Enhancing agent	Adsorbate	Metals eliminated	Adsorption process models	Moisture content (%)	Fixed Charcoal content (%)	References
Neem bark and leaves	HCl, Citric acid and NaOH	Synthetic and real mine used water	Cu^{2+}, Zn^{2+}, Cd^{2+}, Pb^{2+}, Cr^{3+} and Co^{3+}	Langmuir, Freundlich, Temkin, Pseudo - 1st and 2nd orders	3.10	82.25	Hatiya et al. (2022); Adetoro and Ojoawo (2023)
Coconut shell		Real electroplating used water	Zn^{2+} and K^{+}	Freundlich	5.60	49.86	Umerah et al. (2020); Packialakshmi et al. (2023).
Tea dust		Synthetic used water	Cu^{2+} and Ni^{2+}	Langmuir, Freundlich, Pseudo - 1st and 2nd orders	1.90	73.09	Claude et al. (2022)
Orange peel		Real Textile used water	Cu^{2+} and Zn^{2+}	Langmuir, Freundlich, Pseudo - 1st and 2nd orders	8.19	66.41	Kumaraiah et al. (2021); Deshmukh et al. (2022); Naik et al. (2023)
Mango seed		Synthetic used water	Cd^{2+} and Pb^{2+}	Langmuir, Freundlich, Temkin, Dubinin Radushkevich (D-R), and Redlich-Peterson (R-P), Pseudo - 1st and 2nd orders, ΔH, ΔG and ΔS	19.50	61.40	ElNasri et al. (2022); Wang et al. (2022)
Melon seed	NaOH	Synthetic used water	Cu^{2+}, Cd^{2+} and Pb^{2+}	Langmuir, Freundlich, Pseudo - 1st and 2nd orders	7.16	29.96	Khalid et al., 2021; Ahmadi et al. (2023)
Rice husk		dairy used water	Zn^{2+} and Pb^{2+}		8.50	35.00	Naik et al. (2023)
Carica Papaya trunk	HCl	Real mine used water	Co^{3+}, Fe^{2+}, Pb^{2+}	Freundlich, Langmuir, pseudo-second-order, intra-particle diffusion, ΔH, ΔG and ΔS	3.00	69.10	This study.

II. MATERIALS AND METHODS

A. Sampling and analysis

Mine Used Water (MUW) was collected from a marble mining site in Igbeti, Nigeria, in a sealed and sanitized 5-liter plastic container; then moved to Environmental Engineering Laboratory, Ladoke Akintola University of Technology (LAUTECH), Ogbomoso, Nigeria.

B. *Determination of concentrations of contagious metals of MUW*

10 mL of MUW was measured and to speed up the rate of reaction, 10 mL of nitric acid was cautiously poured into it, covered, then placed inside fume cupboard, and heated at a temperature of 100 ˚C for ½ hour. The blend was digested after its elimination from the fume cupboard. The product was made up to 100 mL through the addition of pure water before being filtered and the filtrate analysed by an AAS machine as prescribed by Wiafe et al. (2022), Adetoro and Ojoawo (2023). Each analysis was conducted thrice and the result was recorded in form of mean ± standard deviation.

C. Preparation of Carica Papaya Trunk (CPT) powder

CPT sample obtained from the Teaching and Research farm of LAUTECH. This was chopped and carefully cleaned with pure water for the elimination of all potential impurities. The rinsed CPT sample was dried in the oven at 105 ˚C for a day (Adetoro and Ojoawo, 2023) and then milled into powder, which was stored in a sealed and sanitized 1-litre plastic container.

D. Preparation of Carica Papaya Trunk Enhanced Charcoal (CPTEC)

The prepared CPT powder was poured into rinsed and dried crucibles and then put into a muffle furnace (5X1-1008 Model) at a set temperature of 600 °C. Thereafter, the powdered samples were left inside for an additional one hour. The samples were brought out of the furnace after one hour and spread until they cooled, then rinsed with pure water until the charcoaled sample attained a pH of 7.0. Thereafter, the samples were dried in the oven at 105 °C for 120 minutes and cooled before being activated (Adetoro and Ojoawo, 2023). 50g of the charcoaled CPT was immersed in 500 mL of 0.1 M of HCl acid (i.e. enhancing agent), stirred and immersed for a day, filtered and washed steadily with pure water until the pH level is 7.0, oven-dried at 105 ˚C, and cooled; thereafter, put in a sealed container in preparedness for analysis.

E. Assessment of the CPTEC-HCl adsorbent's properties

Using Fourier Transform Infra-Red (FTIR) and Scanning Electron Microscope (SEM) methods, the functional and surface structural characteristics of the CPTEC-HCl adsorbent were examined.

1) FTIR analysis approach

Through FTIR analysis using an infrared spectrophotometer (Buck Model 530) with wavelength amplitudes of 4000.0 to 400.0 cm^{-1}, the major functional classes that are present in the CPTEC-HCl adsorbent were determined. To press the mixed mixture at 10000.0 kg cm^{-2} for 15 minutes under vacuum, the dried sample (1 mg) and KBr (500.0 mg) (Merck, for spectroscopy) were first ground in a mortar. The major functional classes present on the adsorbent surface were visible from the FTIR wavelength amplitudes.

2) SEM analysis approach

SEM (Model VPFESEM Supra 35VP) was used to take images of the CPTEC-HCl adsorbent sample at 20 µm diameters and 500 x magnifications.

F. Batch adsorption experiments

Six adsorption factors were considered for the batch adsorption experiments namely 0.2 to 1.0g adsorbent quantity (at space of 0.2 g), 50 to 250 rpm shaking rate (at an interval of 50 rpm), 20 to 120 minutes contact time (at 20 minutes interval), granule size (0.075, 0.125, 0.250, 0.425, 1.00 and 2.00 mm), 4 to 10 pH (at a level gap of 2) and 30 to 70 °C temperature (at an interval of 10°C). The varying quantities of the adsorbent (i.e. the HCl-enhanced-CPTEC (CPTEC – HCl) were mixed with 50 ml of the MW sample inside a conical beaker, which was shaken on an orbital shaker at different contact times, granule size, pH, shaking rate and temperature.

The filtrates were subjected to AAS and statistical analyses after being filtered with Whatman filter paper 12.5cm (100 circles) (Adetoro and Ojoawo, 2023). This process was repeated for each of the adsorption factors (i.e. each factor was varied while others remain constant during the experiments). The sorption capacity - q_e (mg/g) and Elimination Efficiency - RE (%) were obtained with Equations 1 and 2 (Ahmadi et al, 2023; Naik et al., 2023).

$$q_e = \frac{(C_o - C_e)\mathrm{V}}{\mathrm{W}} \quad (1)$$

$$\mathrm{RE} = \frac{(C_o - C_e)}{C_o} \text{ x } 100\% \quad (2)$$

Where V is the capacity of the mixture (ml), W is the adsorbent weight (g), $C_{0,}$ and C_e is the primary and stable concentration in the mixture (mg/L).

G. Desorption experiments

Desorption tests were conducted six times (Consecutively with the batch adsorption process) using modified methods of Wang et al. (2022) and Ahmadi et al. (2023) to study the reusability and efficiency of the adsorbent. 0.1M of HCl was used as desorbing agent due to its efficiency (Adetoro et al. 2022). The utilized adsorbent was usually soaked in 15 ml of the desorbing agent for 2 hours, before being centrifuged in an orbital centrifugal machine set at 250 rpm for 20 minutes at room temperature (30 °C), filtered, washed continuously inside BS Sieve 40 (i.e. 0.425mm) with pure water until the pH was between 6.9 and 7.0, dried in the oven at 105 °C, cooled for 120 minutes. The desorbed adsorbent was then used for another batch adsorption study. The results were recorded in form of mean ± standard deviation. The Desorption Efficiency - DE (%) was determined by utilizing equation 3.

$$\mathrm{DE} = \frac{C_d}{C_a} \text{ x } 100\% \quad (3)$$

Where $C_{d,}$ and Ca is the desorbed and adsorbed concentration of contagious metal atom.

H. Isotherm analyses of adsorption

For suitability, equations derived from graphs of batch adsorption data were compared to equations of four selected isotherms (i.e. Freundlich, Dubinin – Radushkevich (D – R), Langmuir, and Temkin isotherms). Freundlich isotherm fitness was determined using Equations 4 and 5, Langmuir isotherm fitness was determined using Equations 6, 7, and 8, D – R isotherm fitness was determined using Equations 9, 10, 11, and 12; while Temkin isotherm fitness was determined using Equations 13 and 14.

$$q_e = KC_e^{1/n} \quad (4)$$

Equation 4 can be expressed linearly as shown in Equation 5 (Naik et al., 2023).

$$\log q_e = \log \mathrm{K} + \frac{1}{\mathrm{n}} \log C_e \quad (5)$$

$$q_e = \frac{q_m . \mathrm{K} . C_e}{1 + \mathrm{K} . C_e} \quad (6)$$

Equation 6 can be expressed linearly as shown in Equation 7 (Claude et al., 2022).

$$\frac{C_e}{q_e} = \frac{1}{q_m . \mathrm{K}} + \frac{C_e}{q_m} \quad (7)$$

$$R_L = \frac{1}{(1 + \mathrm{K} . C_o)} \quad (8)$$

$$q_e = q_m . e^{(-\beta \varepsilon^2)} \quad (9)$$

Equation 9 can be expressed linearly as shown in Equation 10 (Wang et al., 2022).

$$\ln q_e = ln q_m - \beta \varepsilon^2 \quad (10)$$

$$\varepsilon = RTln\left(1 + \frac{1}{C_e}\right) \quad (11)$$

$$\mathrm{E} = 1/\left(\sqrt{2\beta}\right) \quad (12)$$

$$q_e = B . ln(K_t . C_e) \quad (13)$$

Equation 13 can be expressed linearly as shown in Equation 14 (Wang et al., 2022).

$$q_e = \beta ln K_t + \beta ln C_e \quad (14)$$

I. Kinetic analyses of adsorption

The batch adsorption data were studied using three models – Pseudo 1st order, Pseudo 2nd order, and Intra-particle diffusion. Equations 15 and 16 were used for pseudo 1st order kinetic analysis, while Equations 17 and 18 were used for pseudo 2nd order kinetic analysis. The intra-particle diffusion model was examined using Equation 19 (Claude et al., 2022).

$$q_t = q_e(1 - e^{-K_1 t}) \quad (15)$$

Equation 15 can be expressed linearly as shown in Equation 16

$$\log (q_e - q_t) = \log q_e - \frac{K_1}{2.303} \mathrm{t} \quad (16)$$

$$q_t = \frac{K_2 . t . q_e^2}{K_2 . \mathrm{t} . q_e + 1} \quad (17)$$

Equation 17 can be expressed linearly as shown in Equation 18

$$\frac{\mathrm{t}}{q_t} = \frac{1}{K_2 . q_e^2} + \frac{\mathrm{t}}{q_e} \quad (18)$$

$$q_t = K_{diff}\left(t^{\frac{1}{2}}\right) + C \quad (19)$$

J. Thermodynamic analyses of Adsorption

To investigate the adsorption mechanism, three thermodynamic parameters were assessed namely normal enthalpy change (ΔH°); normal entropy change (ΔS°), and normal free energy change (ΔG°). ΔH° and ΔS° were established through modified methods of Rambabu et al. (2021) and Wang et al. (2022).

K. Error functions

The applicability of linear and non-linear regression studies of the suggested adsorption isotherms and kinetics were assessed using two distinct error functions - Sum of Squares of Errors – SSE, and Coefficient of determination – R^2. Equations 20 and 21 were used for SSE and R^2 error functions respectively (Ngakou et al., 2019; Chicco et al., 2021).

$$\mathrm{SSE} = \sum_{i=1}^{n} (q_{ei} - q_{yi})_i^2 \quad (20)$$

$$\mathrm{R}^2 = 1 - \frac{\sum_{i=1}^{n} (q_{ei} - q_{yi})^2}{\sum_{i=1}^{n} (q_x - q_{yi})^2} \quad (21)$$

Where q_{ei}, q_{yi} and q_x is the sorption capacities calculated using the model, experimental, and mean results.

L. Optimization inquiry

In order to acquire the ideal conditions, the adsorption data from batch experiments were subjected to Box Behnken Design (BBD) in the area of Response Surface Methodology (RSM) of Design expert software (version 13) (Stat Ease, 2022).

III. RESULTS AND DISCUSSION

A. Physical attributes of the MUW sample

The MUW sample exhibits water contamination at room temperature as well as ash tincture, a nasty smell, a harsh taste, and darkening from various and peculiar contaminants.

B. The Contagious metals' concentrations in the MUW sample

The concentrations of contagious metals in part per million (mg/L)) present in the pre - and post-treatment of MUW sample are displayed in Table 2 with respective values in decreasing order of Iron (769.85 mg/L) > Lead (51.99 mg/L) > Cobalt (17.23 mg/L). There was increase in their concentrations with increase in year, though not at the same pace. None of the WHO (2022) standards was below the pre-treatment concentrations of the contagious metals. These showed possible pollution of the soil, water bodies, and environment (as a whole) of the study area by the mine used water. WHO (2022) standards were within the ranges of the post-treatment concentrations of Iron and Lead in the MUW, although almost eliminated; whereas cobalt concentration was undetected, thus, indicating its elimination by CPTEC – HCl.

C. Physical attributes of the produced CPTEC-HCl adsorbent

The produced CPTEC-HCl and CPT powder are shown in Figure 1. CPTEC-HCl has black colour and silver-glittering particles, which distinguishes it from other adsorbents.

Table 2: Concentration of contagious metals in the pre - and post-treatment of the MUW sample

Contagious Metal	Concentration in mg / L				
	Pre-treatment			Post-treatment	WHO (2022) Stds.
	Yr. 2020	Yr. 2022	Yr. 2023	CPTEC - HCl	
Cobalt	9.60±0.05	16.57±0.03	17.23±0.02	ND	-
Iron	756.50±0.10	767.09±0.07	769.85±0.04	0.02±0.02	0.3
Lead	45.80±0.06	51.04±0.03	51.99+0.01	0.02+0.01	0.01

ND – Not Detected

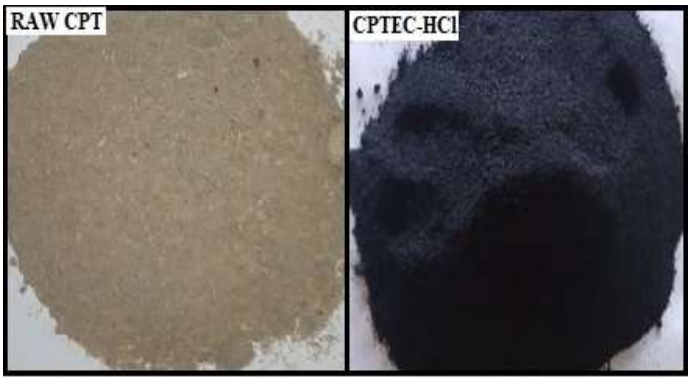

Figure 1: CPTEC produced from raw CPT powder with HCl enhancing agent

D. FTIR analysis findings

The FTIR wavelength amplitudes for the CPT powder and CPTEC-HCl are shown in Figure 2. In order to determine where there are changes in IR amplitudes, the CPT powder FTIR wavelength amplitudes were compared with those of CPTEC - HCl. The FTIR spectra showed that few types of amplitude emerged or vanished, but most were moved lower or higher. The change in amplitude values was caused by the formation of chemical bonds between the functional classes of CPT, confirming the possibility of diverse contaminants being adsorbable by CPT with adequate and satisfying RE based on the FTIR. According to Figure 2 and Table 3, the FTIR spectroscopic investigations of the spectra of the two adsorbents revealed that the IR amplitudes ranged from 3930.6 to 746.3 cm^{-1}. While the IR percent reflectance of CPTEC-HCl is between 0 and 15, that of the raw CPT ranges from 0 to 50.

The differences in IR amplitudes between the CPT and CPTEC-HCl are displayed in Table 3. Bond types were seen to change lower at IR amplitudes of 3787.9, 3657.6, 3232.8, 2919.3, 2762.6, 2544.1 and 2470.6 cm^{-1}. After enhancement, that of 3315.5, 3044.6, 2984.1, 2819.8, and 2614.5 cm^{-1} went higher. With IR amplitudes of 3480.1, 2702.4, and 2402.4 cm^{-1}, bond types vanished, whereas those with IR amplitudes of 3708.5, 3604.0, 3536.3, and 2575.5 cm^{-1} emerged. Bond types changed lower at 2282.3, 2228.9, 2119.2 cm^{-1}, 1767.9, 1675.0, and 1555.2 cm^{-1}. Following then, the values at 1439.1 and 1318.1 cm^{-1} moved higher.

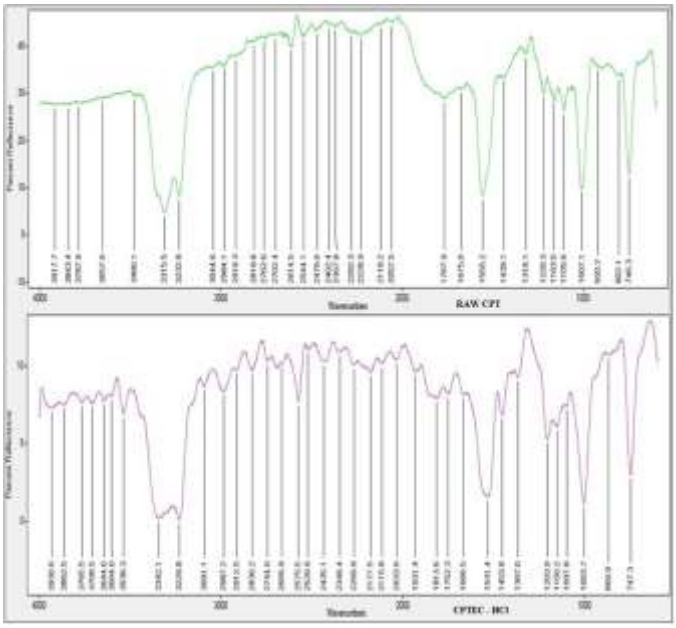

Figure 2: Functional classes - FTIR wavelength amplitudes for raw CPT and CPTEC - HCl

The changes in the FTIR amplitudes demonstrated that CPTEC-HCl would be helpful in the elimination of metals from mine used water, therefore, the changes in the amplitudes supported the effects of enhancement on CPT. In order to improve the functional classes on the adsorbent, enhancement is crucial. According to Wang et al. (2022), among others, the presence of functional classes in the adsorbent, such as alcohols, aldehydes, amines, carboxylic, esters, lactones, ketones, and ether groups, gave it the ability to bind metal ions by donation of an electron pair from these classes to form complexes with the metal ions in solution. Hence, CPTEC-HCl adsorbent may be able to eliminate metal ions from wastewater. The CPTEC-HCl achieved its capability within short IR amplitudes (i.e. 3930.6 to 747.3 cm^{-1}) and percent reflectance (i.e. between 0 and 15). This suggested that CPTEC-HCl might be able to absorb metals more effectively.

E. SEM analysis findings

The surface structure of CPTEC – HCl using SEM is shown in Figure 3. It is observed that its surface was rough, uneven and many pores formed due to the modification using the enhancing agents. There was existence of important pore structures with several irregular pouches scattered over the adsorbents' surfaces as a result of the complex polymer and polysaccharide materials' breakdown when highly heated. The vaporization of evaporative mixtures usually results in adsorbents with well-developed pores. The rise in response in the process of enhancement ended in 'use up' of charcoal, thus developed good pores on the precursors. Because both carbon monoxide (CO) and dioxide (CO_2) constituents of the charcoal were lost, the adsorbents' porosity increased and new pores were formed. The physiochemical treatments led to the production of porous adsorbents. Consequently, as explained by Deshmukh et al. (2022), Ahmadai et al. (2022), and Wattanakornsir et al. (2022), there is an increase in the

Table 3: Changes in the IR amplitudes of the CPT and CPTEC - HCl

RAW CPT		CPTEC - HCl		
IR Amplitude	**Functional Class**	**IR Amplitude**	**Functional Class**	**Remarks**
3917.7		3930.6		Moved higher
3843.4		3862.5		Moved higher
3787.9	Alcohols, Phenols and Carboxylic acids	3765.5	Alcohols, Phenols and Carboxylic acids	Moved lower
		3708.5		Emerged
3657.6	Alcohols, Phenols and	3644.6		Moved lower
		3604		Emerged
		3536.3		Emerged
3480.1	Amides			Vanished
3315.5	Alcohols, Phenols and Carboxylic acids	3342.1	Alcohols, Phenols and Carboxylic acids	Moved higher
3232.8		3229.8		Moved lower
3044.6	Aldehydes, Amides, Carboxylic acids, Ketones and Lactones	3091.1	Amides, Carboxylic acids, Ketones and Lactones	Moved higher
2984.1		2987.2		Moved higher
2919.3		2912.5		Moved lower
2819.8		2830.2		Moved higher
2762.6		2744		Moved lower
2702.4				Vanished
2614.5		2665.9		Moved higher
		2575.5		Emerged
2544.1	Aldehydes, Amides, Carboxylic acids, Ketones and Lactones	2520.9	Aldehydes, Amides, Carboxylic acids, Ketones and Lactones	Moved lower
2470.6		2435.1		Moved lower
2402.4				Vanished
2367.8		2346.4		Moved lower
2282.3	Alkynes and Nitrites	2269.9	Alkynes and Nitrites	Moved lower
2228.9	Alkynes and Nitrites	2177.5	Alkynes and Nitrites	Moved lower
2119.2	Alkynes and Nitrites	2115.8	Alkynes and Nitrites	Moved lower
2057.5		2033.6		Moved lower
		1931.4		Emerged
		1813.6		Emerged
1767.9	Aldehydes, Carboxylic acids, Ketones and Lactones	1752.3	Aldehydes, Carboxylic acids, Ketones and Lactones	Moved lower
1675		1666.5		Moved lower
1555.2	Amides	1531.4	Amides	Moved lower
1439.1		1453.8	Amides	Moved higher
1318.1	Aromatic Amines and primary or secondary OH	1367	Aromatic Amines and primary or secondary OH	Moved higher
1220.3	Aldehydes, Carboxylic acids, Ketones and Lactones	1203.9	Aldehydes, Carboxylic acids, Ketones and Lactones	Moved lower
1163		1150.2		Moved lower
1105.6		1097.8		Moved lower
1007.1		1003.7		Moved lower
920.2				Vanished
802.1	Amines	869.9		Moved higher
746.3	Esters	747.3	Esters	Moved higher

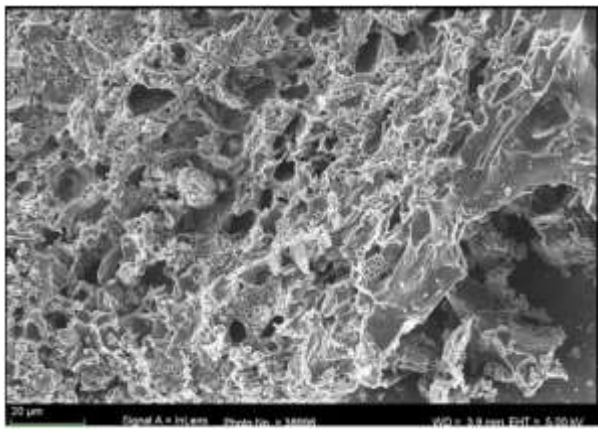

Figure 3: Surface structure of CPTEC – HCl using SEM (Magnification: x 500)

consumption of adsorbate, which is highly important in the adsorption process (es). The surface of the CPTEC-HCl contained numerous irregular pores. These demonstrated the enhancing agent's effectiveness in creating diverse and clearly defined pores on the surface of the precursor, leading to CPTEC-HCl with an extensive porous surface structure.

F. Results of batch adsorption experiments

The percentage removal trends of adsorption factors (adsorbent quantity, contact time, granule size, pH, shaking rate, and temperature) used in the batch adsorption experiments for the contagious metals' removal using CPTEC–HCl adsorbent are shown in Figures 4 to 9. The percentage removal of Co^{3+}, Fe^{2+} and Pb^{2+} observed increased with the increasing sorbent quantity to 0.6 g where optimum Elimination Efficiency (RE) of 99.26 – 100% was achieved (Figure 4). The CPTEC - HCl quantity of 0.6 g has maximum % elimination efficiencies of 100, 100, and 99.26 for Co^{3+}, $Fe^{2+,}$ and Pb^{2+} respectively.

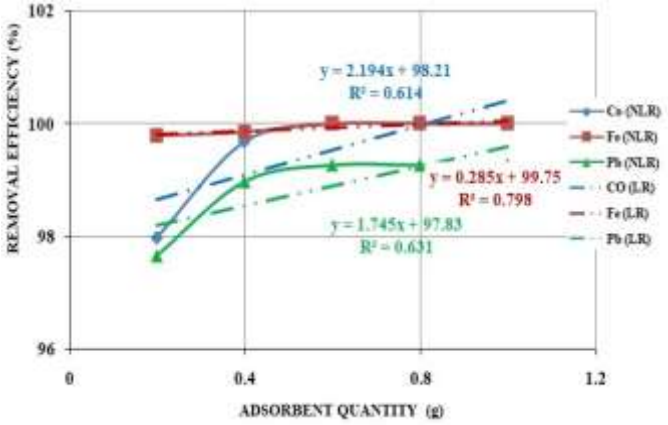

Figure 4: Percentage Removal Trends of Adsorption Quantity utilized for the Experiments (LR – Linear Regression; NLR – Non-Linear Regression).

The increase in shaking rate from 150 to 200 rpm observed remained the same, while RE increased as the shaking rate increased from 50 to 150 rpm as shown in Figure 5. Optimum

RE of 100% for all the contagious metals was attained at a shaking rate of 150 rpm.

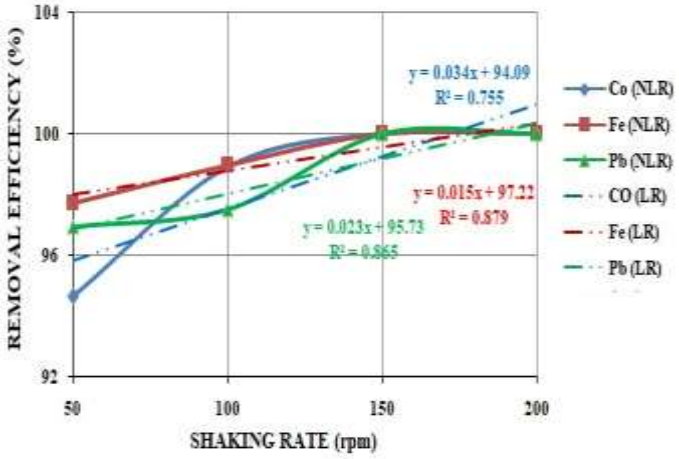

Figure 5: Percentage Removal Trends of Shaking Rate utilized for the Experiments (LR – Linear Regression; NLR – Non-Linear Regression).

RE of Co^{3+}, $Fe^{2+,}$ and Pb^{2+} was seen to rise with the contact time (Figure 6), resulting in peak RE of 100, 99.81, and 98.38% within 60 to 80 minutes for Co^{3+}, $Fe^{2+,}$ and Pb^{2+} respectively.

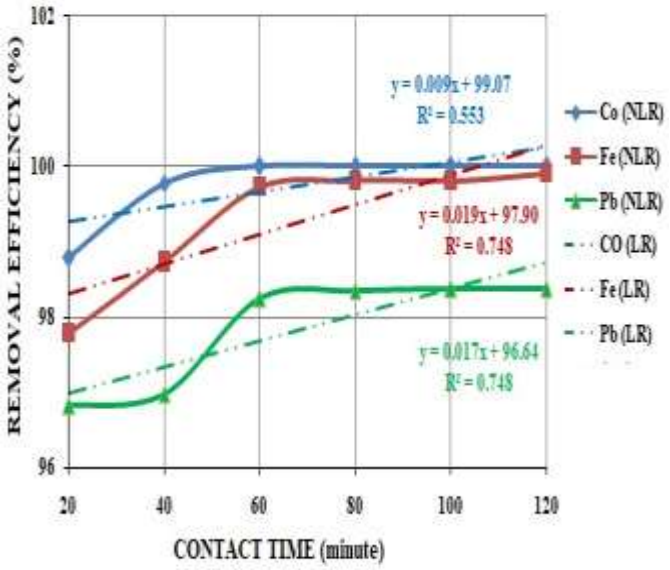

Figure 6: Percentage Removal Trends of Contact Time utilized for the Experiments (LR – Linear Regression; NLR – Non-Linear Regression).

The RE remained the same for the contagious metals from 80 to 120 minutes, which means that none of them was eliminated by the adsorbent. While from 0 to 80 minutes, there was increase in elimination of the contagious metals with increase in contact time as shown in Figure 6. Figure 7 shows that RE of the contagious metals diminished with a rise in granule size, which portrayed that the finer the particles of the adsorbents, the higher the RE. The RE ranged between 94.45 and 100% for all the contagious metals and an optimum RE of 100% was achieved at 0.075 mm.

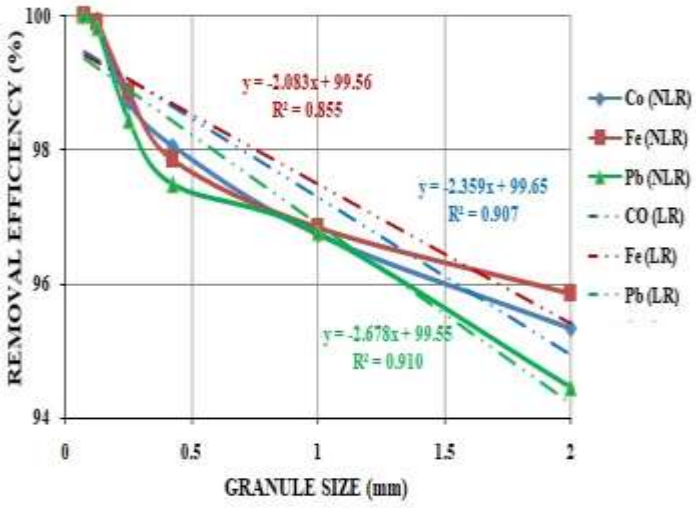

Figure 7: Percentage Removal Trends of Granule Size utilized for the Experiments (LR – Linear Regression; NLR – Non-Linear Regression).

The contagious metals' REs increased and an optimum RE of approximately 100% was reached at pH between 6 and 8 (i.e. change in pH from acidic to alkalinity) for all the contagious metals as portrayed in Figure 8. This could be adduced to the de-protonated adsorbent surface, which results in an attraction between the positively metal cations (Deshmukh et al., 2022). Figure 9 depicts the observed temperature with increase from 30 to 70°C, which resulted in RE reduction. The RE varied from 74.98% (at 70°C) to 99.96% (at 30°C). Optimum RE of 95.75, 99.96, and 98.56% was attained at 30°C for Co^{3+}, Fe^{2+} and Pb^{2+} respectively.

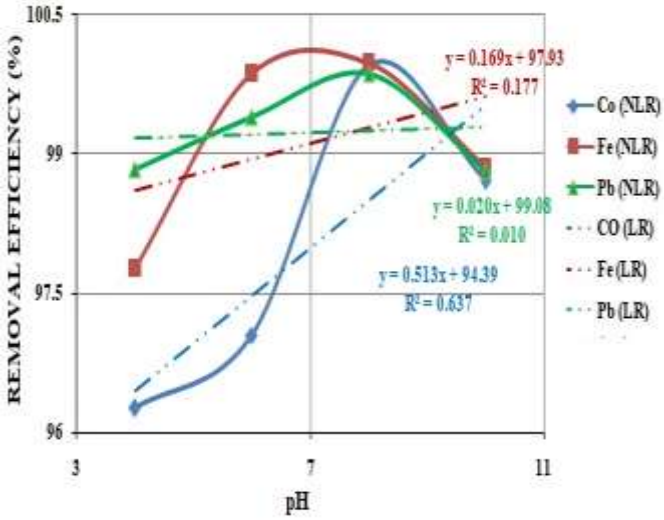

Figure 8: Percentage Removal Trends of pH utilized for the Experiments (LR – Linear Regression; NLR – Non-Linear Regression).

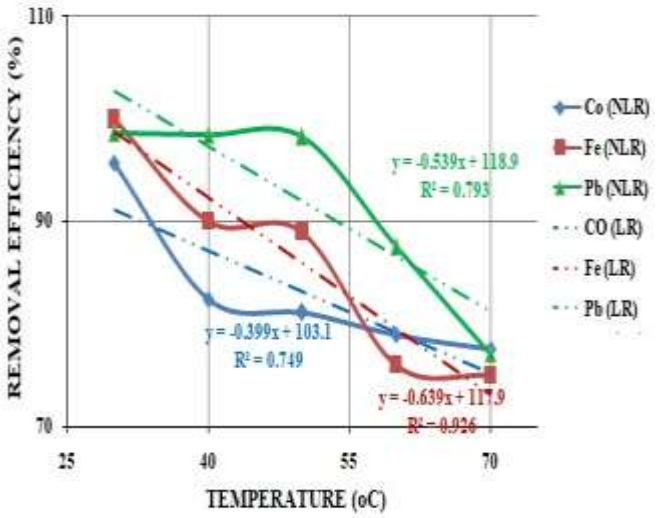

Figure 9: Percentage Removal Trends of Temperature utilized for the Experiments (LR – Linear Regression; NLR – Non-Linear Regression).

G. Summary: Batch Adsorption experiments

In general, all the adsorption factors affected the adsorption capacity and Elimination efficiencies (RE) of the CPTEC - HCl, but varying temperature values had the greatest effect: there was a decrease in metal removal with increase in temperature. The metals removed also decrease as granule size of adsorbent increased. $Co^{3+}$and Fe^{2+} were completely eliminated at around 0.6 g sorbent quantity of CPTEC-HCl, while Pb^{2+} concentration was drastically reduced. The treatments were affected by contact time of 0.0 to 80.0 min and agitation rate of 50.0 to 150.0 rpm (i.e. revolution per minute). The RE recorded for all the adsorption factors proved that enhancement played an important role(s) in achieving elimination of the selected metals in mine used water.

H. Results of desorption experiments

Results of Desorption Efficiency (DE) for the contagious metals in MW treatment using CPTEC – HCl are shown in Table 4. It is observed that all the contagious metals have DE of more than 97% and there was a gradual reduction in adsorption of Co^{3+}, $Fe^{2+,}$ and Pb^{2+} on CPTEC – HCl till the third to the fourth cycle where it remained the same up to the sixth cycle. The RE of the adsorbent was above 97% at optimum conditions throughout the process. The results indicated that CPTEC – HCl has high adsorption efficiency or capacity and revealed its practicability in eliminating the preferred contagious metals from the mine used water (Wang et al., 2022).

I. Results of isotherm analyses of adsorption

The preferred isotherms' results for the findings concerning contagious metals' adsorption mechanism are displayed in Table 5. These portrayed the adsorption mechanism (1/n) to be negative (i.e. irreversible adsorption) for the contagious metals (i.e. Co^{3+}, $Fe^{2+,}$ and Pb^{2+}), thus, frantically chemisorption as expressed by Ojo et al. (2019) and Ahmadi et al. (2022) among others.

Table 4: Desorption Efficiency of CPTEC – HCl in the mine used water treatment

Desorbing Agent	Times	Desorption Efficiency (%)		
		Co^{3+}	Fe^{2+}	Pb^{2+}
0.1M HCl	1	99.91	99.88	99.77
	2	98.89	98.88	99.29
	3	98.11	98.33	97.77
	4	97.38	97.27	97.77
	5	97.38	97.27	97.77
	6	97.38	97.27	97.77

Their adsorption models have low SSE levels for non-linear regression (within acceptable limit i.e. ≤ 5%) when compared with that of their linear regression (not within acceptable limit i.e. >5%), thus, best suited the Freundlich isotherm as corroborated by Hamidi et al., (2012). The R^2 values of their non-linear regression were lower than that of their linear regression. It also showed Fe^{2+} with the highest error values in both linear and non-linear regression analyses to be most predictable as could be seen in its SSE errors values, which are the lowest (Chicco et al., 2021; Turney, 2022). This contradicts the works of Ngakou et al. (2019), which expressed that R^2 cannot truly be used in adjudging the suitability of the adsorption isotherm model because the closer to unity (i.e. R^2 is 1), the more suitable the model (Turney, 2022).

The separation factor, R_L for Co^{3+}, $Fe^{2+}$and Pb^{2+} as shown in Table 5 were irreversible adsorption (i.e. zero or negative) as explained by Ojo et al., (2019) and Ahmadi et al., (2022). Co^{3+} and Fe^{2+} best suited the Langmuir isotherm due to their low non-linear regression SSE values (Hamidi et al., 2012; Chicco et al., 2021) as $Fe^{2+} > Co^{3+} > Pb^{2+}$, which was in agreement with their R^2 predictability. However, their non-linear regression R^2 estimates were lesser when compared with their linear regression. Table 5 also showed that the adsorption energy, E for the contagious metals (i.e. Co^{3+}, $Fe^{2+,}$ and Pb^{2+}) were greater than 16 kJ/Mol, which suggests chemical adsorption according to Ahmadi et al., (2022). The SSE values of their non-linear regression were lesser and within acceptable limits, thus, fitting the D – R isotherm (Hamidi et al., 2012). The adsorption models of Co^{3+} and Fe^{2+} fitted the Temkin isotherm putting into consideration their low non-linear regression SSE values (Hamidi et al., 2012) when compared with their linear regression SSE values. When their R^2 values were also considered, Co^{3+} and Fe^{2+} fitted the isotherm (Chicco et al., 2021; Turney, 2022).

Table 6 depicts the aftermaths of adsorption findings subjected to kinetic models of pseudo 1st and 2nd orders. The experimental and modeled adsorption capacity (q_e) values of the contagious metals were wide apart, thus, none of the contagious metals' adsorption data followed the kinetic form of pseudo 1st order. This opinion was buttressed by their non-

linear regression SSE values, which are not within the acceptable limit (>5%).

Table 5: Summarized Isotherm parameters for the adsorption using CPTEC– HCl

Adsorption Isotherm	Metal	Linear Regression				Non - Linear Regression	
		Parameters		Errors		Errors	
		1/n	K	R^2	SSE	R^2	SSE
Freundlich	Co^{3+}	-3.4223	0.613	0.769	0.331	0.769	0.042
	Fe^{2+}	-0.1677	4425.884	0.975	0.443	0.820	0.006
	Pb^{2+}	-0.4259	9.072	0.985	0.542	0.660	0.021
Langmuir		q_{max}	R_L				
	Co^{3+}	1.595	0	0.843	0.478	0.680	0.041
	Fe^{2+}	14.286	-0.002	0.988	0.434	0.961	0.011
	Pb^{2+}	1.112	-0.022	0.986	0.308	0.128	0.217
D-R		qm	E				
	Co^{3+}	0.6133	7.07E+03	0.769	0.477	0.769	0.018
	Fe^{2+}	169.03	1000	0.023	0.213	0.925	0.039
	Pb^{2+}	0.8082	745.356	0.163	0.350	0.630	0.031
Temkin		K_T	B				
	Co^{3+}	0.15	-7371.53	0.681	0.664	0.681	0.036
	Fe^{2+}	0.4439	-4.058	0.995	0.416	0.998	0.006
	Pb^{2+}	0.446	-225.973	0.103	0.423	0.128	0.048

J. Results of kinetic analyses of adsorption

Table 6: Kinetic models parameters for the adsorption of the contagious metal

Adsorption Kinetics	Metal	Linear Regression				Non -linear Regression	
		Parameters		Errors		Errors	
		q_{yi}	q_{ei}	R^2	SSE	R^2	SSE
Pseudo-1st Order	Co^{3+}	0.800	0.003	0.000	0.438	0.500	0.056
	Fe^{2+}	62.873	0.184	0.029	0.422	0.787	0.088
	Pb^{2+}	3.701	0.156	0.002	0.419	0.721	0.084
Pseudo-2nd Order	Co^{3+}	0.800	0.800	0.993	0.442	1.000	0.036
	Fe^{2+}	62.873	62.873	0.993	0.410	1.000	0.006
	Pb^{2+}	3.701	3.701	0.995	0.393	1.000	0.033

The results of linear and non-linear retrogression analyses indicated that adsorption processes of contagious metals perfectly followed the kinetic form of pseudo 2nd order albeit correlation coefficient mostly in all cases tending towards unity (i.e. R^2 is 1). Comparatively, the latter demonstrated to be most suitable for the investigation owing to less SSE estimates (i.e. within the acceptable limit - ≤ 5) of the contagious metals' models. In addition, adsorption capacities obtained from both experimental (q_{yi}) and modeled (q_{ei}) results were coequal for all the selected contagious metals (Table 6). The kinetic model of pseudo 2nd order has a basis in the reality of the sorption rate being governed by chemical sorption. At the beginning of the process, the sorption sites at the adsorbents' surface were free and could easily bind the

contagious metal ions. The sites bit by bit got concentrated and the ion's concentration at the boundary decreased in a gradual manner as well as the adsorption rate with time as expressed by Adetoro and Ojoawo (2023).

Table 7 shows the findings of the model of intra-particle diffusion for the contagious metals' adsorption. It was observed that the values of intercept C, the models' impetus parameter vary between 0.797 and 62.901. Fe^{2+} and Co^{3+} have the topmost and under most estimates of intercept C respectively. A higher cut-off means greater adsorption and presence of other mechanisms are included along with intra-particle diffusion of Fe^{2+} as expressed by Wang et al. (2022).

K. Summary: isotherm and kinetic analyses of adsorption

All the adsorption data of the contagious metals (Co^{3+}, Fe^{2+} and Pb^{2+}) best suited Freundlich and D-R isotherms and Pseudo 2nd order kinetic models, while Langmuir and Temkin isotherm models best fitted into Co^{3+} and Fe^{2+} adsorption data. In general, non – linear regression (NLR) analyses of the adsorption data proved to be better because of lower SSE values (< 5%) and corresponding R^2 tending towards unity (or perfect prediction of the outcomes) when compared to the linear regression (LR) analyses, which has higher SSE values (> 5%) and R^2.

L. Results of thermodynamic analyses of adsorption

The findings of thermodynamic analyses of adsorption for the contagious metals are depicted in Table 8. The negative and positive estimates of respective normal enthalpy change (ΔH°) and entropy change (ΔS°) denoted that the processes were favourable, feasible, natural, and suggest physical nature with weak forces of attraction; while positive ΔS values portray irregular increase of the uncertainty at the band particles betwixt solid-solution during the mechanism. Pore size's step-up and adsorbent surfaces' enhancement resulted in a higher adsorption capacity during hotness. Moreover, increase in negatives values of ΔG between 30 and 50 °C of Pb^{2+} adsorption means reduced natural adsorption process; while its decrease in Co^{2+} and Fe^{2+} adsorption depicted increase in spontaneous adsorption process as the temperature increases (Ojo et al., 2019; Wang et al., 2022).

M. Results of optimization studies

When the adsorption data of the contagious metals were subjected to optimization studies for optimal performance using Design expert software (version 13), the adsorption optimization solution was 0.516 g of adsorbent quantity, 146.576 rpm shaking rate, 51.718 minutes contact time, 0.028 mm granule size, pH of 6.969 and 30 °C temperature. This solution resulted in 100 % Elimination efficiencies (RE) for all the contagious metals (i.e. Co^{3+}, Fe^{2+} and Pb^{2+}). The standard error of the mean ranged between 0.013 (i.e. Fe^{2+}) and 0.260 % (Co^{3+}), which clearly showed that it is less than the 5 % significance level. Comparison of CPTEC – HCl with adsorbents produced from other agricultural bio-materials - Neem bark and leaves (Hatiya et al., 2022; Adetoro and Ojoawo, 2023), Coconut shell (Umerah et al., 2020; Packialakshmi et al., 2023), Orange peel (Kumaraiah et al., 2021; Deshmukh et al., 2022 and Naik et al., 2023), Mango seed (ElNasri et al., 2022; Wang et al., 2022) etc in elimination of contagious metals from wastewater also showed it to be among the best and its Elimination efficiency is equivalent to that of the commercial enhanced charcoal, thus, can be utilized as its replacement in wastewater treatment.

Table 7: Parameters of the model of intra-particle diffusion for the contagious metals

Contagious Metals	Parameters	
	C	K_{diff}
Co^{3+}	0.797	3.00E-04
Fe^{2+}	62.901	9.00E-04
Pb^{2+}	3.715	-0.001

Table 8: Adsorption thermodynamic parameters for the contagious metals' adsorption

Temp (°C)	Desc.	Co^{3+}	Fe^{2+}	Pb^{2+}
30	R^2	0.749	0.926	0.793
	ΔS	857.173	980.221	988.535
	ΔH	-0.854	-1.610	-1.358
	ΔG	-7846.678	-19708.875	-10645.950
40	ΔS	857.173	980.221	988.535
	ΔH	-0.882	-1.663	-1.403
	ΔG	-4026.090	-5706.253	-10735.476
50	ΔS	857.173	980.221	988.535
	ΔH	-0.910	-1.716	-1.447
	ΔG	-3913.126	-5600.834	-10801.035
60	ΔS	857.173	980.221	988.535
	ΔH	-0.939	-1.769	-1.492
	ΔG	-3651.479	-3185.197	-5382.314
70	ΔS	857.173	980.221	988.535
	ΔH	-0.967	-1.822	-1.537
	ΔG	-3536.700	-3129.874	-3458.641

IV. CONCLUSION

The research established that CPTEC produced from CPT using HCl enhancing agent is dark in colour with silver shining particles. Enhancement plays an important role in enhancing the functional classes (alcohols, aldehydes, amines, carboxylic, esters, lactones, ketones, phenols and ether groups) on the adsorbent, which gave it the ability to bind metal ions, hence was able to eliminate the selected contagious metals (Co^{3+}, Fe^{2+}, and Pb^{2+}) from mine used water. The adsorption processes carried out on the mine used water using the produced CPTEC-HCl were highly influenced by the selected adsorbent factors (i.e. adsorbent quantity, contact time, granule size, pH, shaking rate and temperature) and majorly irreversible adsorption (frantically chemisorptions) for all the contagious metals with Elimination efficiency of 100 %. All the contagious metals data largely followed models of Freundlich and D – R isotherms and also best-suited model of Pseudo 2nd order kinetics. Non-Linear Regression (NLR) analysis (using the SSE and R^2 error functions) demonstrated to be excellent means of studying the models of the adsorption isotherms and kinetics of the selected contagious metals. The adsorption processes of the contagious metals according to the thermodynamic studies were favourable, feasible, and natural. All the contagious metals (i.e. Co^{3+}, Fe^{2+} and Pb^{2+}) were eliminated completely using 0.516 g of the adsorbent with 0.028 mm granule size at 146.576 rpm, 51.718 minutes, pH of 6.969 and 30 °C temperature. The CPTEC - HCl proved to be better and excellent alternative to commercial enhanced charcoal in real-world wastewater treatment (especially mine used water) when compared with other agricultural adsorbents.

AUTHOR CONTRIBUTIONS

E. A. Adetoro: Conceptualization, Methodology, Software, Resources, Field work, Laboratory analysis, Data collation, Validation, Writing –original draft. **S. O. Ojoawo:** Data collation, Methodology, Software, Resources, Field work, Laboratory analysis, validation. Writing - reviewing and editing.

ACKNOWLEDGEMENT

This research was conducted in the Department of Civil Engineering, Faculty of Engineering and Technology, Ladoke Akintola University of Technology, Ogbomoso, Nigeria.

FUNDING

This research did not receive any specific grant from funding agencies in the public, commercial, or not-for-profit sectors.

REFERENCES

Adetoro, A. E. and Ojoawo, S. O. (2023). Remediation of heavy metal ions from mining wastewater using *Azadirachta indica* bark adsorbent. *International Journal of Environment and Waste Management*, 34(3): 340 - 366.

Ahmadi, H.; S. S. Hafiz; H.; Sharifi; N. N. Rene; S. S. Habibi and S. Hussain. (2022). Low cost biosorbent (Melon peel) for effective removal of Cu(II), Cd(II),and Pb(II) ions from aqueous solution. *Case Studies in Chemical and Environmental Engineering*, 6(10-242): 1-12.

Badamasi, H.; U. F. Hassan; H. M. Adamu and N. M. Baba. (2021). Evaluation of heavy metals pollution status of the groundwater around Riruwai mining area, Kano State, Nigeria. *European Journal of Environment and Earth Sciences*, 2(3):234-245.

Chicco, D.; M. J. Warrens and G. Jurman. (2021). The coefficient of determination R-squared is more informative than SMAPE, MAE, MAPE, MSE and RMSE in regression analysis evaluation. *PeerJ Comput. Sci.*, 7(e623): 34-45.

Claude, N. J.; L. Shanshan; J. Khan; W. Yifeng; H. Dongxu and L. Xiangru. (2022). Waste tea residue adsorption coupled with electrocoagulation for improvement of copper and nickel ions removal from simulated wastewater. *Scientific Reports*, 12(3519): 1-11.

Deshmukh, S.; N. S. Topare; S. Raut-Jadhav; P. V. Thorat; V. A. Bokil and A. Khan. (2022). Orange peel activated carbon produced from waste orange peels for adsorption of methyl red. *AQUA — Water Infrastructure, Ecosystems and Society*, 71(12): 1351 - 1363.

ElNasri, N.A.; N. A. Wadidi; A. A. Idris; S. K. Woldemicheal and S. I. A. Elhaj. (2022). Properties of natural adsorbent prepared from two local Sudanese agricultural wastes mango seeds and dates'stones and their uses in removal of contamination from fluid nutrient. *Bulletin of the National Research Centre*, 46(79): 1–7.

Hatiya, N.A.; A. S. Reshad and Z. W. Negie. (2022). Chemical modification of neem (azadirachta indica) biomass as bioadsorbent for removal of Pb^{2+} ion from aqueous wastewater. *Adsorption Science and Technology*, ID 7813513: 1–8.

Hadzi, G. Y. (2022). Effect of mining on heavy metals toxicity and health risk in selected rivers of Ghana. *Intechopen*, 102093: 1270-1295.

Hamidi, A. E.; S. Arsalane and M. Halim. (2012). Kinetics and isotherm studies of copper removal by brushite calcium phosphate: Linear and non-linear regression comparison. *E-Journal Chem*, 9: 1532–1542.

Idibie, C. A.; E. Omo-Udoyo and P. Embelegha. (2021). Process Optimization and Kinetics Study of Locally Produced Activated Carbon from *Carica Papaya* Seeds on Methylene Blue Adsorption. *FUPRE Journal of Scientific and Industrial Research*, 5, (2): 21 - 29.

Khalid, W.; A. Ikram; M. Rehan; F. A. Afzal; S. Ambreen; M. Ahmad; A. Aziz and A. Sadiq. (2021). Chemical composition and health benefits of melon seed: A review. *Pakistan Journal of Agricultural Research*, 34(2): 309 - 317.

Karn, R.; N. Ojihab; S. Abbas and S. Bhugrad. (2021). A review on heavy metal contamination at mining sites and remedial techniques. *IOP Conference Series: Earth and Environmental Science*, 796 (012013): 23-34.

Kumaraiah, P.H.; P. Karanth; M. A. Sobande; E. A. Adetoro and S. O. Ojoawo. (2021). Biosorption of Colour, Copper and Zinc in Textile Wastewater using Carbonized Orange Peels. *LAUTECH Journal of Civil and Environmental Studies*, 6: 90–106.

Minga, J. C.; F. J. Elorza; R. Rodriguez; A. Iglesias and D. Esenarro. (2023). Assessment of water resources pollution associated with mining activities in the Parac subbasin of the Rimac River. Water, 15 (965): 1-11.

Naik, L.; M. R. Kumar and T. B. Narsaiah. (2023). Removal of heavy metals (Cu and Ni) from wastewater using rice husk and orange peel as adsorbents. *Materials Today: Proceedings*, 72(1): 92 – 98.

Natania, K.; J. F. Setiadi; Hardoko and D. D. Rosa. (2022). Correlation between bitterness removal and functional properties of *Papaya* (*Carica papaya* L.) leaves. *Indonesian Food Science and Technology Journal (IFSTJ)*, 5 (2): 71 – 75.

Ngakou, C. S.; G. S. Anagho and H. M. Ngomo. (2019). Non-linear Regression Analysis for the Adsorption Kinetics and Equilibrium Isotherm of Phenacetin onto Activated Carbons. *Current Journal of Applied Science and Technology*, 36: 1–18.

Ojo, T. A.; A. T. Ojedokun and O. S. Bello. (2019). Functionalization of powdered walnut shell with orthophosphoric acid for Congo red dye removal. *Particle Science and Technology*, 37: 74–85.

Packialakshmi, S.; B. Anuradha; K. Nagamani; D. J. Sarala and S. Sujatha. (2023). Treatment of industrial wastewater using coconut shell based activated carbon. *Materials Today: Proceedings*, 81(2): 1167 – 1171.

Rambabu, K.; A. Thanigaivelan; G. Bharath; N. Sivarajasekar; F. Banat and P. L. Show. (2021). Biosorption potential of Phoenix dactylifera coir wastes for toxic hexavalent chromium sequestration. *Chemosphere*, 268 (128809): 1-9.

Samrot, A. V.; S. Saigeetha; C. Mun; S. Abirami; K. Purohit; P. J. J. Cypriyana; T. S. Dhas; L. Inbathamizh and S. Kumar. (2021). Utilization of *Carica papaya* latex on coating of SPIONs for dye removal and drug delivery. *Scientific Reports*, 11(24511): 34-44.

Stat Ease (2022). Design expert software version 13. Stat Ease Inc., Minneapolis, US. Available online at http://www.statease.com. Accessed on June 28, 2023.

Turney, S. (2022). Coefficient of Determination (R^2) - calculation and interpretation. Accessed on July 08, 2023.

Umerah, O.; D. Kodali; S. Head; S. Jeelani and K. Rangari. (2020). Synthesis of carbon from waste coconut and their application as filler in bioplast polymer filaments for 3D printing. *Composites Part B: Engineering*, 202(108428): 1-10.

Wang, Q.; Y. Wang; Z. Yang; W. Han; L. Yuan; L. Zhang and X. Huang. (2022). Efficient removal of Pb (II) and Cd (II) from aqueous solutions by mango seed biosorbent. *Chemical Engineering Journal Advances*, 11 (100295): 1-15.

Wattanakornsir, A.; P. Rattanawan; T. Sanmueng; S. Satchawan; T. Jamnongkan and P. Phuengphai. (2022). Local fruit peel biosorbents for lead (II) and cadmium (II) ion removal from waste aqueous solution: A kinetic and equilibrium study. *South African Journal of Chemical Engineering*, 42: 306–317.

World Health Organization - WHO. (2022). Guidelines for drinking-water quality. 4th edition incorporating the 1st and second addenda. *Encyclopedia of Earth Sciences Series*,126- 127.

Wiafe, S.; E. A. Yeboah; E. Boakye and S. Ofosu. (2022). Environmental risk assessment of heavy metals contamination in the catchment of small-scale mining enclave in Prestea Huni-Valley District, Ghana. *Sustainable Environment*, 8 (1): 1-11.